



ORIGINAL ARTICLE

# Comparison between exact and approximate methods for geometrically nonlinear analysis prescribed in design standards for steel and reinforced concrete structures

*Comparação entre métodos exato e aproximados de análise geometricamente não linear prescritos em normas de estruturas de aço e de concreto armado*

Laís De Bortoli Lecchi<sup>a</sup> Walnório Graça Ferreira<sup>b</sup> Paulo Manuel Mendes Pinheiro da Providência e Costa<sup>c</sup> Arlene Maria Cunha Sarmanho<sup>a</sup> <sup>a</sup>Universidade Federal de Ouro Preto – UFOP, Departamento de Engenharia Civil, Ouro Preto, MG, Brasil<sup>b</sup>Universidade Federal do Espírito Santo, UFES, Departamento de Engenharia Civil, Vitória, ES, Brasil<sup>c</sup>Universidade de Coimbra, Instituto de Engenharia de Sistemas e Computadores de Coimbra – INESC Coimbra, Departamento de Engenharia Civil, Coimbra, Portugal

Received 28 December 2020

Accepted 13 April 2021

**Abstract:** Current practices in structural engineering demand ever-increasing knowledge and expertise concerning stability of structures from professionals in this field. This paper implements standardized procedures for geometrically nonlinear analysis of steel and reinforced concrete structures, with the objective of comparing methodologies with one another and with a geometrically exact finite element analysis performed with Ansys 14.0. The following methods are presented in this research: Load Amplification Method, from NBR 8800:2008; the  $\gamma_z$  coefficient method, from NBR 6118:2014; the P-Delta iterative method and the  $\alpha_{cr}$  coefficient method, prescribed in EN 1993-1-1:2005. A bibliographic review focused on standardized approximate methods and models for consideration of material and geometric nonlinearities is presented. Numerical examples are included, from which information is gathered to ensure a valid comparison between methodologies. In summary, the presented methods show a good correlation of results when applied within their respective recommended applicability limits, of which, Eurocode 3 seems to present the major applicability range. The treated approximate methods show to be more suitable for regular framed structures subjected to regular load distributions.

**Keywords:** global stability analysis, approximate nonlinear analysis, P-Delta iterative method,  $\alpha_{cr}$  coefficient, ANSYS.

**Resumo:** As práticas atuais em engenharia estrutural exigem cada vez mais conhecimento e expertise, em relação à estabilidade de estruturas, por parte dos profissionais da área. Este artigo implementa procedimentos normativos de análise de segunda ordem aproximada de estruturas de aço e concreto armado, com o objetivo de comparar as metodologias aproximadas entre si e com uma análise de elementos finitos geometricamente exata realizada no Ansys 14.0. Os seguintes métodos são tratados nesse trabalho: Método da Amplificação dos Esforços Solicitantes, da NBR 8800:2008; o método do Coeficiente  $\gamma_z$ , da NBR 6118:2014; o método P-Delta iterativo e o método do Coeficiente  $\alpha_{cr}$ , da EN 1993-1-1:2005. É apresentada uma revisão bibliográfica a respeito dos métodos normativos e como são tratadas as não linearidades de materiais e geométricas. Exemplos numéricos estão incluídos, de onde são extraídas as informações para a comparação entre as metodologias. Em resumo, os métodos apresentados mostram boa correlação de resultados quando aplicados dentro dos respectivos limites de aplicabilidade recomendados, dos quais, o Eurocódigo 3 aparenta ter a maior faixa de aplicabilidade. Os métodos aproximados tratados mostram ser mais adequados para estruturas apertadas regulares e sujeitas à carregamentos regulares.

Corresponding author: Laís De Bortoli Lecchi. E-mail: [laislecchi@gmail.com](mailto:laislecchi@gmail.com)

Financial support: None.

Conflict of interest: Nothing to declare.



This is an Open Access article distributed under the terms of the Creative Commons Attribution License, which permits unrestricted use, distribution, and reproduction in any medium, provided the original work is properly cited.

**Palavras-chave:** análise de estabilidade global, análise não linear aproximada, método P-Delta iterativo, coeficiente  $\alpha_{cr}$ , ANSYS.

**How to cite:** L. B. Lecchi, W. G. Ferreira, P. M. M. P. Providência e Costa, and A. M. C. Sarmanho, "Comparison between exact and approximate methods for geometrically nonlinear analysis prescribed in design standards for steel and reinforced concrete structures," *Rev. IBRACON Estrut. Mater.*, vol. 15, no. 1, e15101, 2022, <https://doi.org/10.1590/S1983-41952022000100001>

## 1 INTRODUCTION

### 1.1 Initial considerations

In recent decades, structural engineering and civil construction underwent significant technological advancements, which resulted in the reduction of weight and overall improvement of structural systems, in turn allowing the construction of buildings with heights previously deemed impossible. As such, the development of methods and analysis software to ensure the safety of these buildings became a necessity.

Engineering design standards include procedures for first and second order structural analyses. A first order analysis is characterized by determining the equilibrium equations of structures in their undeformed condition. In this type of analysis, structures are assumed to undergo small displacements that bear no effect on the developed internal forces. Alternatively, in a second order geometric analysis (or nonlinear), the equilibrium equations refer to the structure in the deformed configuration, resulting in a system of nonlinear equations. This approach is required when the applied loads interact with the resulting displacements inducing significant additional internal forces [1]. It is worth noting that nonlinear analyses may be performed considering either small or large strains theories – the former case is considered in this paper. To evaluate second order effects, it is necessary to consider the different types of nonlinearity, namely, geometric and material nonlinearities. The nonlinear behavior of a structure significantly affects displacements and internal forces.

Publications by Horne [2], Wood et al. [3] and LeMessurier [4], [5] were fundamental for the development of practical design methods for multi-story buildings, namely by introducing an approximate method for considering the  $P-\Delta$  effect. In Brazil, studies conducted by Franco [6], Franco and Vasconcelos [7] and Vasconcelos [8], focused on the assessment of second order effects in reinforced concrete buildings, culminated in the  $\gamma_z$  coefficient method, currently detailed in NBR 6118:2014 [9] for the structural design of reinforced concrete structures.

This paper presents four approximate methods: the Load Amplification Method (MAES, in Portuguese), originally presented in ANSI/AISC 360-16 [10], and subsequently adopted by NBR 8800:2008 [11] for the structural design of steel buildings; the  $\gamma_z$  coefficient prescribed in NBR 6118:2014 [9] and used for the classification of the structure and also as a design factor for the horizontal loads; the equivalent lateral force method (iterative  $P$ -Delta), adopted by NBR 8800:1986 [12], which adds fictitious lateral loads to the horizontal loads; and the method prescribed in the European standard EN 1993-1-1:2005 [13] for the design of steel structures, that uses the  $\alpha_{cr}$  coefficient to classify a structure according to its sensitivity to second order effects.

### 1.2 Material nonlinearity

Material nonlinearity is defined as a nonlinear relationship between stress and strain on a given material. This issue can come from: partial yielding of steel sections, also accentuated by the presence of residual stresses; the influence of semirigid connections; creep and cracking on reinforced concrete elements, for example.

The standards NBR 8800:2008 [11], NBR 6118:2014 [9] and ANSI/AISC 360-16 [10], allow the approximate treatment of material nonlinearities, characterized by a reduction of the axial and flexural stiffnesses of structural elements.

### 1.3 Geometric nonlinearities

An effect of geometric nonlinearity is the lack of proportionality between applied loads and resulting displacements [14]. This type of nonlinear behavior results from the interaction between the load and the displacements. In frames, two different types of displacement are relevant: the inter-story drift, which causes the  $P-\Delta$  effect, and the curvature of the elements, which causes the  $P-\delta$  effect. However, the global imperfections (initial drift) and the local imperfections (initial curvature) are not nonlinear effects.

Design standards commonly include simplified methods for modelling geometric nonlinearities. The Brazilian standard NBR 8800:2008 [11], for instance, determines that, in structures subjected to load combinations composed exclusively of vertical forces, initial geometric imperfections are considered by introducing notional forces equivalent to 0.3% of the value of dead loads. Alternatively, ANSI/AISC 360-16 [10] also allow the use of notional forces, but with a magnitude of 0.42% for first order analyses and 0.2% for the direct analysis method, a method for assessment of overall system structural stability (it also includes initial material imperfections, by adjustments in stiffness).

The method prescribed in NBR 6118:2014 [9] accounts for the misalignment of structural elements, and, for cases with a load amplification factor  $\gamma_z > 1.1$ , such a factor is taken as  $0.95\gamma_z$ . For the design of frames, Eurocode 3 [13] allows the amplification of horizontal loads if  $\alpha_{cr} \geq 3$ , along with the inclusion of theoretical lateral loads even in cases with horizontal load combinations. However, the inclusion of notional forces when horizontal external loads are present is only applicable if these forces are inferior to 15% of the loads attributed to the weight of structural elements.

#### 1.4 Approximate methods for second order analysis

The inelastic second order analysis can properly describe the actual behavior of a structure, since it includes the plastic behavior of materials [15]. However, the relatively complex formulation of this refined approach is a complicating factor. As such, simplified procedures may be used to perform second order analyses. Computational alternatives for  $P-\Delta$  analyses were being developed since the 1980s, such as the procedure introduced by Rutenberg [16]. Wilson and Habibullah [17] also presented an approximate computational method for determining second order effects in frames subjected to horizontal loads.

LeMessurier [5] presented an interesting formulation for approximate nonlinear analysis that relies on the amplification of first order effects, which eventually served as a base for the development of other methods such as MAES ( $B_1 - B_2$ ).

As stated by Ziemian [15], approximate methods must be used with caution since they may be inadequate for amplifying bending moments in regions connecting beams and columns. It is worth noting that these methodologies are only recommended for framed structures with uniform loads [18].

Dória et al. [19] assert that the ratio of first to second order displacements ( $\Delta_2 / \Delta_1$ ) may not be the best approach for quantifying second order effects in structures. Additionally, the  $B_2$  coefficient, used to approximate  $\Delta_2 / \Delta_1$ , might lead to incorrect results when analyzing second order effects. As an alternative, the above authors recommend the use of the  $\alpha_{cr}$  coefficient adopted by Eurocode 3 [13], as a more adequate indicator of the importance of second order effects in structures.

## 2 APPROXIMATE METHODS FOR GEOMETRICALLY NONLINEAR ANALYSIS

### 2.1 Method prescribed in NBR 8800:2008

#### 2.1.1 Introduction

The Load Amplification Method implements the amplification factors  $B_1$  and  $B_2$ . This approach was first introduced by SSRC (Structural Stability Research Council) and subsequently adopted by AISC in 1986 [20].

$B_1$  amplifies the loads to account for the  $P-\delta$  effect (local), while  $B_2$  treats the  $P-\Delta$  effect (global). These coefficients may be used for the analysis of reticulated structures consisting of structural elements with uniform geometry and stiffness, provided  $B_2 \leq 1.4$  [21]. The  $B_2$  coefficient must be determined for each pavement, and it is not adequate for analyzing structures with split story levels [15].

The  $B_1 - B_2$  method consists in decomposing the structural model in two parts, as shown in Figure 1. The first submodel, traditionally referred to as *nt*, meaning “no translation” – maintains the original load configuration, but is now subjected to fictitious horizontal restraints in each pavement to prevent horizontal translation. The second submodel – named *lt*, for “lateral translation” – is exclusively subjected to the aforementioned horizontal restraints reactions, but with opposite direction. After the subdivision, both models are subjected to an elastic first-order analysis.

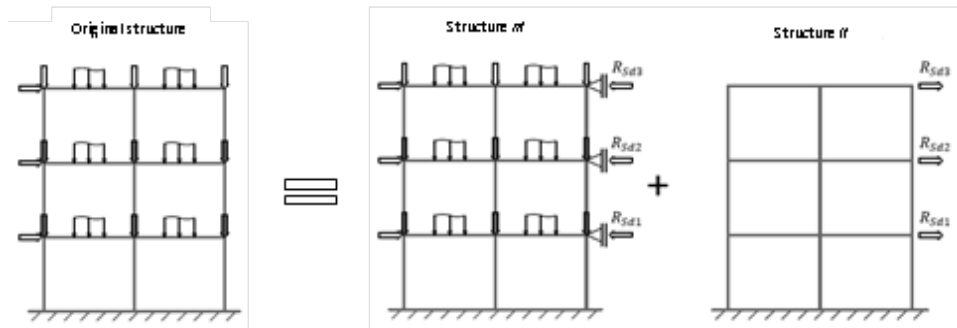


Figure 1 – Original structure divided into two models. Source: Badke-Neto and Ferreira [22].

### 2.1.2 Adjustments to stiffness

According to NBR 8800:2008 [11] the flexural and axial stiffnesses of structures with high sensitivity to second order effects must be reduced to  $0.8EI$  and  $0.8EA$ , respectively. ANSI/AISC-360-16 [10] includes an additional reduction factor  $\tau_b$ , and stipulates that the reduced stiffnesses must be used to determine strength and stability limits only. In other words, the reduced properties are not used to obtain displacements, deflections or periods of vibration.

### 2.1.3 Initial Geometric imperfections

NBR 8800:2008 [11] determines that the initial global geometric imperfections may be accounted for by either considering an inter-story drift equal to  $h/333$ , where  $h$  is the story height, or by imposing notional forces equivalent to 0.3% of the gravitational loads acting on a given story subjected to combinations without lateral loads, in other words, it provides a minimum destabilizing effect [23].

### 2.1.4 Classification of the structure

The Brazilian standard [11] classifies a structure according to its susceptibility to displacements. If the ratio between the second-order displacement  $\Delta_2$  and first-order displacement  $\Delta_1$  is less than or equal to 1.1, the structure is defined as having small susceptibility. Alternatively, if the condition  $1.1 < \Delta_2 / \Delta_1 \leq 1.4$  is satisfied, the structure is of medium susceptibility. If neither of these conditions are met, a high susceptibility to displacements is attributed to the structure. The  $B_2$  coefficient is considered an acceptable approximation of the ratio  $\Delta_2 / \Delta_1$ , if  $\Delta_2 / \Delta_1 \leq 1.4$  [11], or  $\Delta_2 / \Delta_1 \leq 1.5$ , in ANSI/AISC-360-16 [10] case. It is worth noting that ANSI/AISC-360-16 [10] does not include this classification (small, medium, or high susceptibility).

### 2.1.5 Methodology from annex D of NBR 8800:2008

Given an adequately defined load combination, the axial load  $N_{sd}$  and the bending moment  $M_{sd}$  acting on each floor are given by Equations 1 and 2, respectively.

$$M_{sd} = B_1 M_{nt} + B_2 M_{lt} \tag{1}$$

$$N_{sd} = N_{nt} + B_2 N_{lt} \tag{2}$$

where  $M_{nt}$  and  $N_{nt}$  are the design bending moment and axial force, respectively, obtained via elastic first-order analysis of submodel  $nt$ . Similarly,  $M_{lt}$  and  $N_{lt}$  are the design bending moment and axial force obtained from an elastic first-order analysis of submodel  $lt$ . The shear force is determined with an elastic first-order analysis of the original model (which is equivalent to the sum of submodels  $nt$  and  $lt$ ).

### 2.1.6 The $B_1$ coefficient

For an unbraced member in the plane of bending under consideration, NBR 8800:2008 [11] defines  $B_1$  as:

$$B_1 = \frac{C_m}{1 - \frac{|N_{Sd1}|}{N_e}} \geq 1.0 \quad (3)$$

$C_m$  is an equivalent moment factor given by  $C_m = 0.60 - 0.40(M_1 / M_2)$ , where  $M_1$  and  $M_2$ , calculated from a first-order analysis, are the smaller and larger moments, respectively, at the ends of that member.  $M_1 / M_2$  is positive when the member is bent in reverse curvature and negative when bent in single curvature.  $N_{Sd1}$  is the design axial force on the member, obtained from a first-order analysis,  $N_{Sd1} = N_{nt} + N_{lt}$ .  $N_e$  is the critical elastic buckling load of the member in the direction of bending, given by Euler's critical load  $N_e = \pi^2 EI / L^2$ , where  $E$  is the modulus of elasticity,  $I$  is the moment of inertia of the cross-section and  $L$  is the length of the member.

### 2.1.7 The $B_2$ coefficient

A detailed deduction of  $B_2$  is given e.g. in Souza et al. [24]. NBR 8800:2008 [11] defines  $B_2$  as:

$$B_2 = \frac{1}{1 - \frac{1}{R_S} \frac{\Delta_h}{h} \frac{\sum N_{Sd}}{\sum H_{Sd}}} \quad (4)$$

where  $\sum N_{Sd}$  is the total dead load acting on the analyzed story.  $\sum H_{Sd}$  is the total shear force on this story, obtained from the original structure or from submodel  $lt$  (Figure 1).  $\Delta_h$  is the relative displacement between the top and bottom pavements of the story, obtained from the original structure or submodel  $lt$ .  $h$  is the ceiling height of the story.  $R_S$  is an adjustment coefficient, associated to the type of present bracing and it values 0,85, for frame bracing systems and 1,0, for all others.

## 2.2 Method prescribed in NBR 6118:2014: The $\gamma_z$ coefficient

### 2.2.1 Introduction

NBR 6118:2014 [9] classifies framed structures as either fixed nodes or movable nodes. When ratio of second-order to first-order internal forces is larger than 10%, i.e.  $\gamma_z > 1.1$ , the structure is sensitive to second order effects. Otherwise, fixed nodes are considered. The  $\gamma_z$  coefficient serves two purposes: Classification of the structure and second order amplification of horizontal loads, determining the total horizontal load acting on the system.

### 2.2.2 Material nonlinearity according to NBR 6118:2014

Material nonlinearities, commonly present in reinforced concrete structures and having a significant influence on second order effects, must always be accounted for [25], by means of reducing the stiffness of each structural element.

### 2.2.3 Initial geometric imperfections according to NBR 6118:2014

Initial global geometric imperfections are included in the form of an initial out of plumbness of the columns, or the corresponding angle  $\theta_a$ , as shown in Figure 2 (Eurocode 3 [13] provides similar expressions):

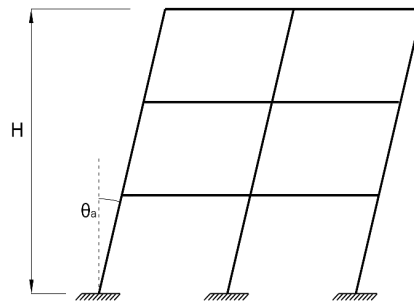


**Figure 2** – Initial out of plumbness. Source: Adapted from NBR 6118-2014 [9].

where:

$$\theta_1 = \frac{1}{100\sqrt{H}} \tag{5}$$

$$\theta_a = \theta_1 \sqrt{\frac{1+1/n}{2}} \tag{6}$$

in which:

$$\theta_{1,min} = 1/300 ; \theta_{1,max} = 1/200 ;$$

$H$  is the total height;  $n$  is the total number of columns lines of the frame.

The drift in angular form ( $\theta_a$ ) can be converted into an equivalent force  $H_i = \theta_a F_{vi}$ , in which  $F_{vi}$  is the load acting on a given floor [26].

According to NBR 6118-2014 [9], if 30% of the tipping moment caused by the incidence of wind is larger than the tipping moment caused by horizontal out of plumbness, the latter is neglected. Alternatively, if the moment caused by wind is less than 30% of the horizontal out of plumbness moment, the former is neglected. In any other scenario, the two types of tipping moment are considered in the load combination, not necessarily respecting the condition imposed by  $\theta_{1,min}$ .

Initial local geometric imperfections in reinforced concrete structures are included during structural design procedures for each column, using either the method of approximate curvature or the method of approximate stiffness.

### 2.2.4 The $\gamma_z$ coefficient

In 1991, Franco and Vasconcelos presented the  $\gamma_z$  coefficient for the first time, in the paper “Practical Assessment of Second Order Effects in Tall Buildings” [7]. The complete deduction of  $\gamma_z$  is detailed in Souza et al. [24], and it is ultimately determined by:

$$\gamma_z = \frac{1}{1 - \frac{\Delta M_{tot,d}}{M_{1,tot,d}}} \tag{7}$$

where  $M_{1,tot,d}$  is the tipping moment and  $\Delta M_{tot,d}$  is the sum of the products between vertical forces acting on the structure and the respective horizontal displacements.

In essence, the only difference between  $\gamma_z$  and  $B_2$  is the factor  $1/R_s$ , present in the formula for  $B_2$ , and attributed to the type of bracing on the structure. According to section 15.7.2 of NBR 6118:2014 [9], if  $\gamma_z > 1.1$ , the horizontal loads must be multiplied by the factor  $0.95\gamma_z$ . This procedure is valid only for  $\gamma_z \leq 1.3$ .

The fact that  $\gamma_z$  is defined only once for the entire structure is an interesting practical advantage, especially if compared to other methods such as MAES. However, as stated by Avakian [27], the  $\gamma_z$  coefficient does not yield acceptable results when implemented in frames with non-rigid connections. Additionally, Silva [14] concluded that the  $\gamma_z$  method gives poor results for frames with lateral bracing.

### 2.3 The lateral equivalent force method or iterative P-Delta method

NBR 8800:1986 [12] prescribes in, Annex L, an approximate method for performing elastic second-order analyses, designated as iterative P-Delta method. This method, also adopted by AISC and by the Canadian standard CSA-S16.1 [28], consists of adding the actual horizontal loads of the structure to fictitious lateral loads obtained iteratively (see Figure 3). At the end of this process, the total load on the structure is obtained, since the fictitious lateral loads induce a behavior similar to second-order effects.

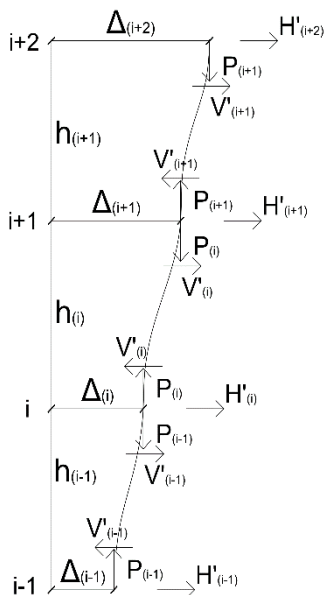


Figure 3 – Displacements and fictitious loads in multi-story buildings. Source: Adapted from NBR 8800:1986 [12].

Every analysis in this method is first-order. Initially, horizontal displacements are calculated for each floor. This step is followed by determining the fictitious shear force in each story  $i$  using Equation 8:

$$V'_i = \frac{\sum P_i}{h_i} (\Delta_{i+1} - \Delta_i) \tag{8}$$

where  $V'_i$  is the fictitious shear force in floor  $i$ ;  $\sum P_i$  represents the summation of axial forces acting on the columns of floor  $i$ ;  $h_i$  is the height of the floor under analysis and  $\Delta_{i+1}, \Delta_i$  indicate the horizontal displacement of floors  $i+1$  and  $i$ , respectively. Since displacements differ in each floor, the shear forces  $V'_i$  are not in equilibrium. This unbalanced equation induces the fictitious lateral force  $H'_i$ , as shown in Figure 3, calculated with Equation 9.

$$H'_i = V'_{i-1} - V'_i \tag{9}$$

On the next iteration, initial loads must be once again applied to the structure, including the obtained forces  $H'_i$ , resulting in new displacements. Consequently, a new lateral force  $H'_i$  must be added to the initial loading in the following iteration. This procedure is repeated until the difference between displacements in two consecutive iterations is smaller than a convergence criterion established beforehand.

Bernuzzi and Cordova [29] affirm that, if convergence is slow, demanding six or seven iterations, it indicates that the loading configuration is considerably close to the elastic limit or that the structure is excessively flexible. Moreover, the process may be interrupted when the convergence factor is equal to 5%. The NBR 8800:1986 [12] does not mention reductions of axial and flexural stiffnesses to account for material nonlinearity.

## 2.4 Methodology from the European standard for steel structures EN 1993-1-1: 2005

### 2.4.1 Initial considerations

The standard EN 1993-1-1:2005 [13], Eurocode 3 in this paper, indicates that first-order analyses may be used if the effect of the displacements is not relevant, i.e. provided Equations 10 and 11 are met.

$$\alpha_{cr} = \frac{F_{cr}}{F_{ed}} \geq 10, \text{ for elastic analysis} \quad (10)$$

$$\alpha_{cr} = \frac{F_{cr}}{F_{ed}} \geq 15, \text{ for plastic analysis} \quad (11)$$

where  $\alpha_{cr}$  is a factor by which design loads would have to be increased to result in elastic instability;  $F_{ed}$  is the vertical design load acting on the structure and  $F_{cr}$  is the critical elastic buckling load. If  $\alpha_{cr} \geq 10$ , the structure is considered to have low sensitivity to second order effects, which is equivalent to the fixed node classification of NBR 6118:2014 [9].

It is important to note that this method is only applicable if the framed structure under analysis is subjected to equally spaced gravitational and destabilizing loads and is composed of uniform structural elements. Since the method is based on a linear elastic analysis, second-order effects are induced by amplifying horizontal loads. This procedure is executed by applying a  $\beta$  coefficient (Equation 12), which is a function of  $\alpha_{cr}$ .

$$\beta = \frac{1}{1 - \frac{1}{\alpha_{cr}}} \quad (12)$$

An alternative for determining  $\alpha_{cr}$  via elastic buckling analysis is given in Equation 13, which is based on a method for standard framed systems proposed by Horne [2]. It is worth noting that this proportionality relation is valid for small displacement theory. For multi-story structures, the factor must be calculated for each story, but only the smallest value is ultimately used. This method is applicable if  $\alpha_{cr} \geq 3$ .

$$\alpha_{cr} = \frac{H_{ed}}{V_{ed}} \cdot \frac{h}{\delta_{H,ed}} \quad (13)$$

In which  $H_{ed}$  : is the total horizontal force;  $V_{ed}$  : is the total vertical load applied on the horizontal surface of a given story under analysis;  $h$  : is the height of the building and  $\delta_{H,ed}$  : is the displacement of the level above, calculated for a structure subjected only to the horizontal loads  $H_{ed}$ .

It is possible to note similarity between  $\beta$ ,  $\gamma_z$  and  $B_2$ .  $\beta$ , as well as  $\gamma_z$ , does not depend on the factor  $1/R_g$ . In essence, the difference among the procedures for determining each of these coefficients lays in how each method accounts for initial material and geometric imperfections.



## 2.4.2 Initial geometric imperfections

### 2.4.2.1 Initial global geometric imperfections

Initial global geometric imperfections are included in the analysis by applying a global initial sway imperfection angle  $\varphi$  to the structure, which may be neglected if  $H_{ed} \geq 0.15V_{ed}$  (clause 5.3.2(4) of Eurocode 3 [13]). In Eurocode 3, the angle  $\varphi$  is given by:  $\varphi = \varphi_0 \alpha_h \alpha_m$ , where  $\varphi_0$  is the basic value ( $\varphi_0 = 1/200$ );  $\alpha_h$  is a reduction coefficient related to the height  $h$  of the structure in meters ( $\alpha_h = 2/\sqrt{h}$ , with  $2/3 \leq \alpha_h \leq 1$ ) and  $\alpha_m$  is a reduction coefficient related to the number of columns,  $\alpha_m = \sqrt{0.5(1+1/m)}$  and  $m$  is the number of columns on a given row. It is easy to notice that these expressions are identical to those prescribed by in NBR 6118-2014 [9].

Alternatively, the horizontal drift may be replaced by the equivalent lateral force shown in Figure 4 [30], given by:

$$F' = \varphi V_{ed} \tag{14}$$

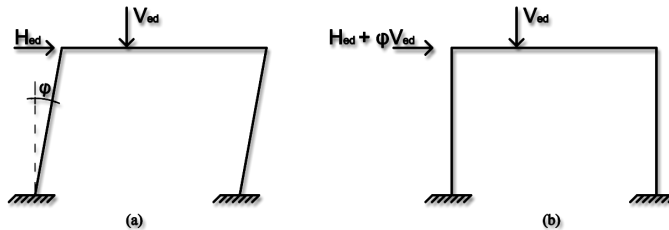


**Figure 4** – Consideration of initial global imperfection by (a) initial sway; (b) equivalent lateral force (notional force). Source: Adapted from [30].

### 2.4.2.2 Initial local geometric imperfections

Clause 5.3.2(6) of Eurocode 3 stipulates that the global analysis of structures sensitive to second-order effects must include initial local imperfections in members subjected to compression in which a) at least one end is not free to rotate and b)  $N_{ed} > (F_{cr} / 4)$ . Initial local imperfections may also be replaced by equivalent forces.

## 2.4.3 Adjustments to stiffness associated to material nonlinearity

Eurocode 3 does not require a reduction of the modulus of elasticity  $E$ , as other standards do.

## 3 NUMERICAL EXAMPLES

### 3.1 Example 1: Single span single story frame

Figure 5a shows a single span single story plane frame (adapted from [30]), along with its dimensions and the numbering of nodes and bars (underlined). The structure is subjected to the loads shown in Figure 5b. The load magnitudes displayed already represent the least favorable load combination. All columns are composed of the profile HEA280, while beams feature section IPE500. The modulus of elasticity of steel is taken as  $E = 200\text{ GPa}$ .

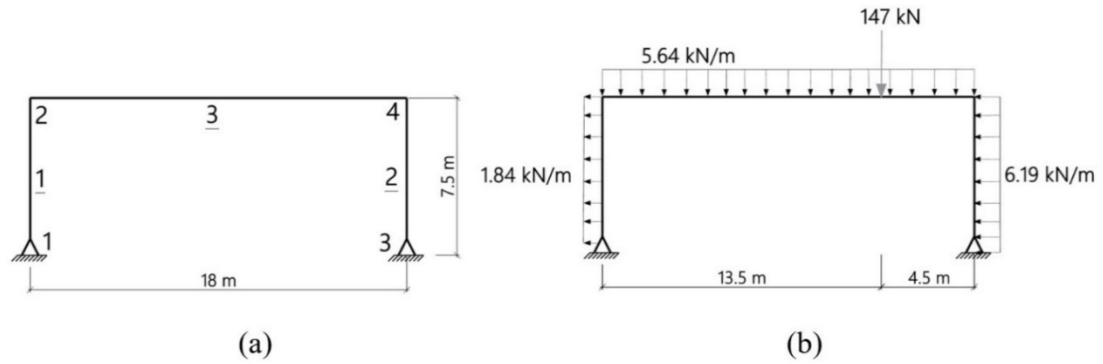


**Figure 5** - Single-span single-story frame: (a) dimensions and numbering (b) design loads. Source: Authors (2020).

A first-order elastic analysis was performed to determine the displacements and internal forces, on Ftool 4.0 program. The structure was also modeled in a finite-element based analysis software (Ansys 14.0), in order to perform an exact geometrically nonlinear analysis. Each bar was modelled with a mesh of 10 elements BEAM188 (a two-node linear finite strain beam based on Timoshenko beam theory). Initial geometric imperfections (notional forces) were not included on this model with the least favorable load combination, according to the rules and recommendations of each standard. Material nonlinearity was considered by adjusting the members stiffness by means of a reduction of the modulus of elasticity ( $0.8E$ ), for the case of MAES, the  $\gamma_z$  coefficient and on Ansys. The Newton-Raphson method was used to perform the nonlinear analysis.

### Summary of results

Table 1 summarizes the results obtained with each method:

**Table 1** – Summary of results. Source: Authors (2020).

	Elastic analysis	$B_1 - B_2$ Method	$\gamma_z$ coefficient	P-Delta method	Eurocode method	Ansys
Amplification coefficients	-	$B_1 = 1.00$ $B_2 = 1.20$	$\gamma_z = 1.20$	$\frac{\Delta_2}{\Delta_1} = 1.13$	$\beta = 1.13$	$\Delta_2 / \Delta_1 = 1.21$
$\Delta_4$ . node 4 [cm]	15.22	18.96	22.11	17.18	20.40	24.3
Bending moment Column 2 [kNm]	96.8	63.9	75.7	75.4	75.6	64.2
Axial force Column 2 [kN]	-148.5	-144.8	-145.9	-146.1	-146.0	-146.3
Shear force Column 2 [kN]	36.1	36.1	38.0	33.3	36.3	31.4

### 3.2 Example 2: Eleven story two span frame

Figure 6 shows a steel frame with eleven stories and two spans (adapted from [14]), along with its dimensions and numbering of nodes and bars (underlined). The columns feature welded profiles and the beams rolled profiles, as shown in Table 2. The modulus of elasticity of steel is taken as  $E = 200\text{ GPa}$ .

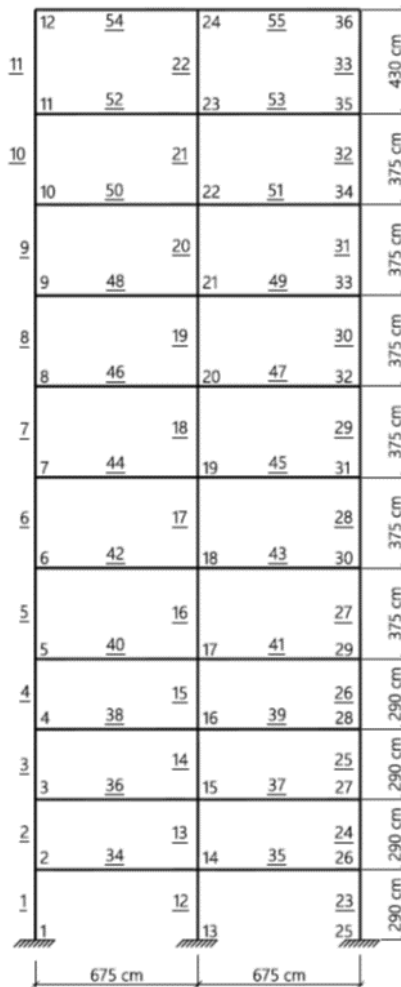


Figure 6 – Frame with eleven stories and two spans: Dimensions and numbering. Source: Authors (2020)

Table 2 – Profiles used for columns and beams (dimensions in mm). Source: Authors (2020)

Bar number	Profile
1 - 4; 23 - 26	PS 500 x 300 x 16 x 8
12 - 15	PS 500 x 300 x 19 x 9,5
5 - 7; 16 - 18; 27 - 29	PS 500 x 300 x 12,5 x 8
8 - 11; 19 - 22; 30 - 33	PS 500 x 300 x 9,5 x 6,5
34 - 55	W 530 x 66

Figure 7a and 7b illustrates the design horizontal and vertical loads, respectively. The values displayed correspond to the least favorable load combination of the structure. The group of loads shown in Figure 7 is designated as  $Q_R$  (set of reference loads).

An exact geometrically nonlinear analysis of the structure was performed using a finite element analysis program (Ansys 14.0). Each bar was modelled with a mesh of 20 elements BEAM188 (a two-node linear finite strain beam based on Timoshenko beam theory). Initial geometric imperfections (notional forces) were included on this model (with the least favorable load combination) only for the Eurocode 3 method, according to the rules and recommendations of each standard.

Material nonlinearity was again considered by adjusting the members stiffness by means of their reduction ( $0.8EI; 0.8EA$ ), for the case of MAES, the  $\gamma_z$  coefficient and on Ansys, when the related amplification factors were greater than 1.1. Five

simulations were performed, progressively increasing the reference load  $Q_R$  by a factor  $n$ . Tables 3, 4, 5 and 6 present the obtained results.

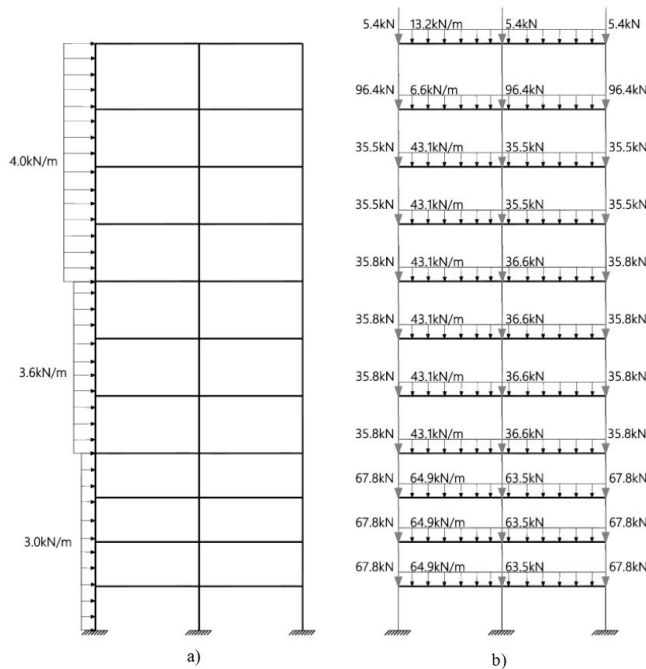


Figure 7 – Design loads applied to the structure: a) horizontal loads and b) vertical loads. Source: Authors (2020)

Table 3 – Final multiplier  $B_2$ . (bold font values exceed the applicability limit of the method). Source: Authors (2020).

$n$	Coefficient $B_2$										
	1° floor	2° floor	3° floor	4° floor	5° floor	6° floor	7° floor	8° floor	9° floor	10° floor	11° floor
1	1.06	1.10	1.10	1.09	1.10	1.09	1.07	1.05	1.03	1.02	1.01
2	1.16	1.30	1.30	1.26	1.30	1.25	1.20	1.15	1.10	1.05	1.03
3	1.27	<b>1.52</b>	<b>1.52</b>	<b>1.44</b>	<b>1.52</b>	<b>1.43</b>	1.33	1.25	1.15	1.08	1.04
4	1.40	<b>1.83</b>	<b>1.84</b>	<b>1.70</b>	<b>1.84</b>	<b>1.67</b>	<b>1.49</b>	1.36	1.21	1.10	1.06
5	<b>1.55</b>	<b>2.31</b>	<b>2.34</b>	<b>2.04</b>	<b>2.33</b>	<b>2.00</b>	<b>1.70</b>	<b>1.50</b>	1.28	1.13	1.07

Table 4 – Multiplier coefficients  $\gamma_Z$ ,  $\alpha_{cr}$  and  $\beta$ . (bold font values exceed the applicability limit of the methods) Source: Authors (2020).

$n$	$B_1$	$\gamma_Z$	$\alpha_{cr}$	$\beta$
1	1.0	1.08	12.68	1.09
2	1.0	1.18	6.19	1.19
3	1.0	1.29	4.23	1.31
4	1.0	<b>1.43</b>	3.17	1.46
5	1.0	<b>1.61</b>	<b>2.54</b>	<b>1.65</b>

Table 5 – Ratio of initial to final displacements  $(\Delta_2 / \Delta_1)$ . obtained with the P-Delta method. Source: Authors (2020).

$n$	$(\Delta_2 / \Delta_1)$ - P-Delta method.										
	1° floor	2° floor	3° floor	4° floor	5° floor	6° floor	7° floor	8° floor	9° floor	10° floor	11° floor
1	1.10	1.12	1.13	1.13	1.14	1.15	1.16	1.17	1.18	1.20	1.22
2	1.20	1.18	1.18	1.18	1.18	1.18	1.18	1.18	1.17	1.17	1.17
3	1.27	1.29	1.29	1.29	1.28	1.27	1.27	1.25	1.24	1.23	1.23
4	1.41	1.43	1.42	1.42	1.41	1.40	1.38	1.36	1.35	1.34	1.33
5	1.56	1.59	1.59	1.59	1.57	1.55	1.53	1.51	1.49	1.47	1.46

**Table 6** - Ratio of initial to final displacements ( $\Delta_2 / \Delta_1$ ) obtained with Ansys. Source: Authors (2020).

n	$(\Delta_2 / \Delta_1)$ - Ansys.											
	1° floor	2° floor	3° floor	4° floor	5° floor	6° floor	7° floor	8° floor	9° floor	10° floor	11° floor	
1	1.07	1.08	1.08	1.08	1.08	1.08	1.08	1.08	1.07	1.07	1.07	1.07
2	1.15	1.17	1.18	1.18	1.18	1.17	1.17	1.16	1.15	1.15	1.14	1.14
3	1.27	1.28	1.29	1.29	1.29	1.28	1.27	1.26	1.25	1.24	1.23	1.23
4	1.39	1.42	1.43	1.43	1.43	1.42	1.40	1.38	1.36	1.35	1.39	1.39
5	1.54	1.58	1.60	1.60	1.60	1.59	1.56	1.53	1.51	1.49	1.48	1.48

The horizontal top floor displacement (node 36) is shown in Figure 8. The geometrically exact analysis performed with Ansys gives the larger displacement values, followed by  $\gamma_z$ , Eurocode method, P-Delta and MAES.

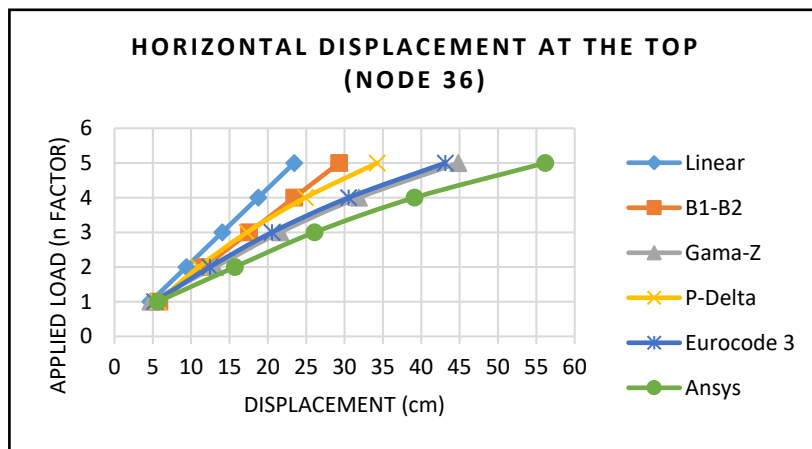


**Figure 8** – Top floor displacement at node 36. Source: Authors (2020)

For each method, internal forces were analyzed on column 27 (5<sup>th</sup> floor), where the highest values of load multipliers are observed, and column 33 (11<sup>th</sup> floor), which presents the smallest values. Figures 9 through 14 show the obtained results.

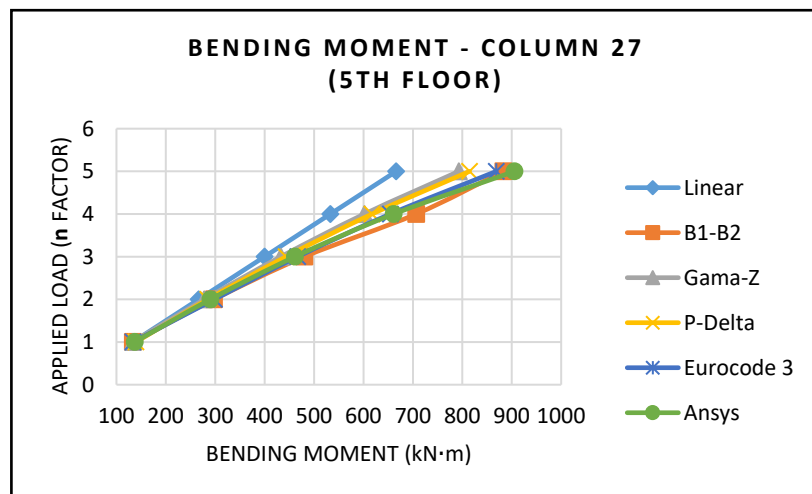


**Figure 9** – Load - bending moment relationship for column 27. Source: Authors (2020).

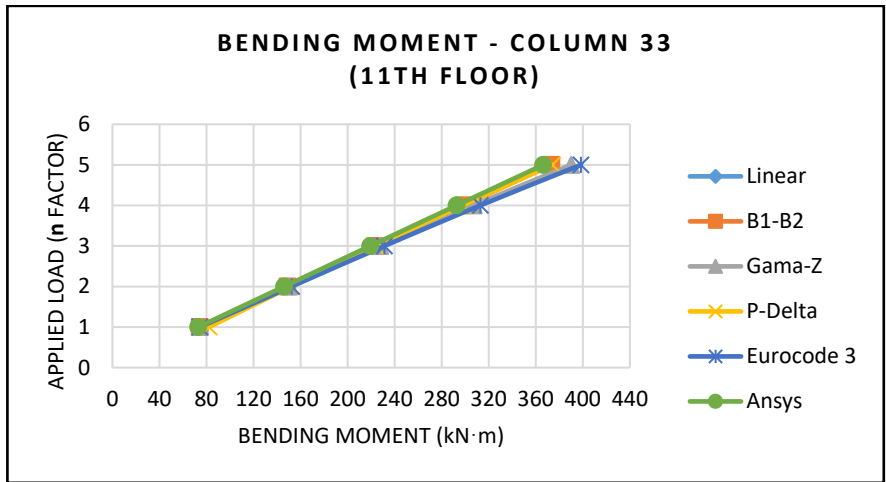


Figure 10 - Load - bending moment relationship for column 33. Source: Authors (2020).

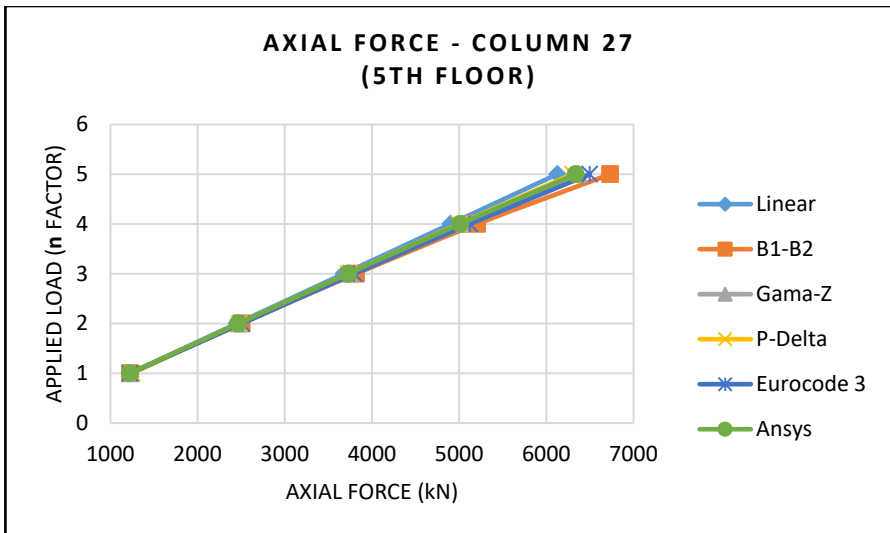


Figure 11 - Load - axial force relationship for column 27. Source: Authors (2020).

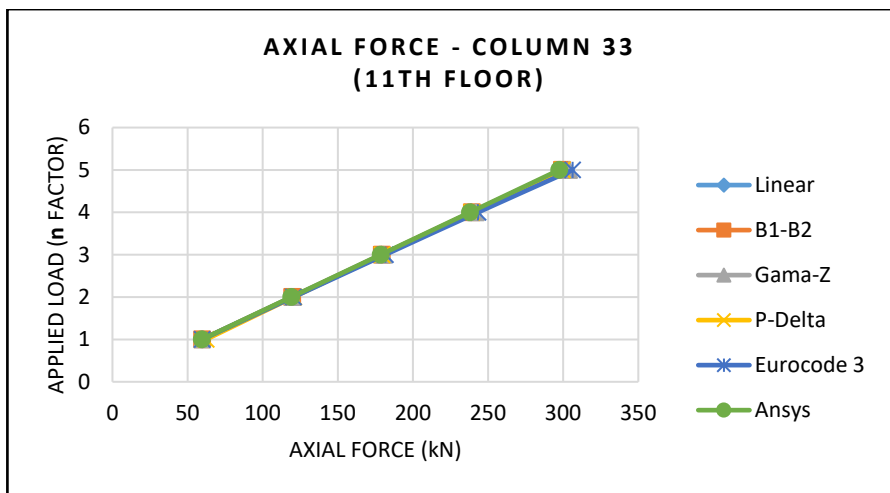


Figure 12 - Load - axial force relationship for column 33. Source: Authors (2020).

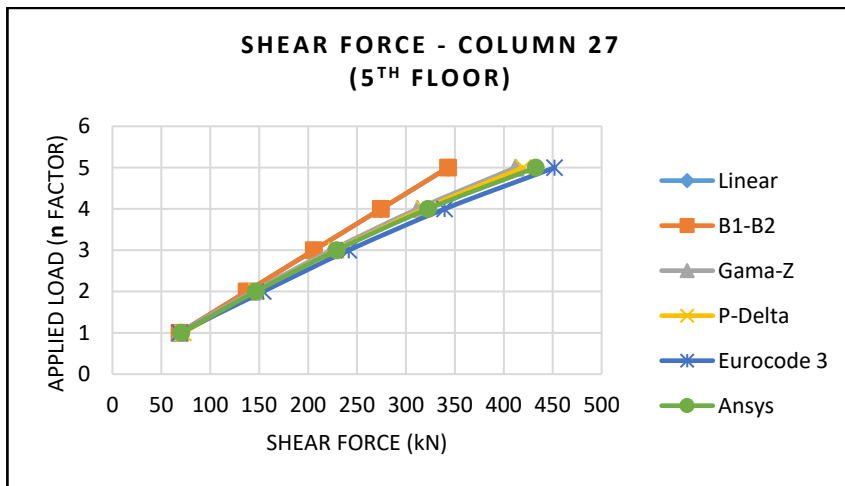


Figure 13 - Load - shear force relationship for column 27. Source: Authors (2020).

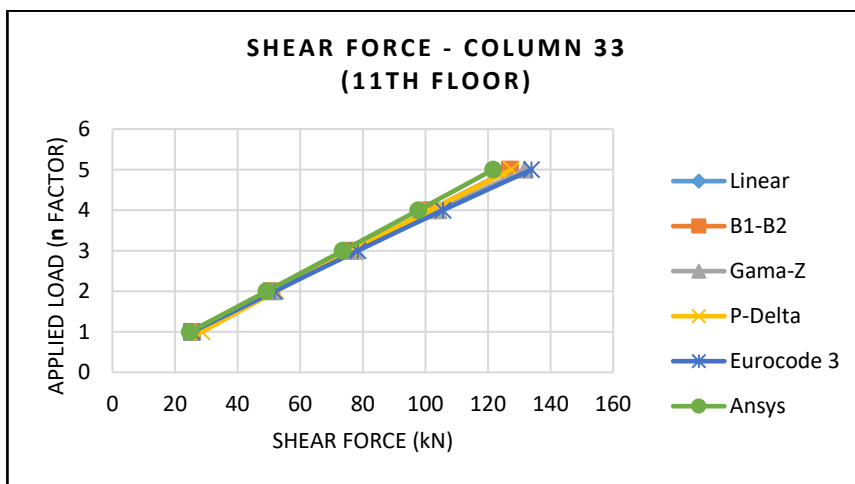


Figure 14 - Load - shear force relationship for column 33. Source: Authors (2020).

## 4 RESULTS AND DISCUSSIONS

### 4.1 Example 1: Single span single story frame

Concerning the analysis of displacements, the exact analysis performed with Ansys presents the most conservative results, followed by  $\gamma_z$  coefficient and the Eurocode method, known for overestimating horizontal loads. However, according to ANSI/AISC-360-16 [10], the amplified displacements should not be taken as an accurate depiction of reality, and here they only serve as a parameter for qualitative analysis.

Results for bending moments obtained via the  $B_1 - B_2$  method are the closest to Ansys. Remaining methods yielded similar results between them and differ from the exact analysis by approximately 17.5%.

All methods present similar results for axial forces, with a maximum observed difference of 1%. This is not the case for the values of shear force, which show significant difference between the exact analysis and the other methods, the  $\gamma_z$  method presenting the largest value of maximum shear force acting on the structure.

### 4.2 Example 2: Frame with eleven stories and two spans

Figure 9 (Load - bending moment relationship), for column 27, indicates that the approximate methods show good correlation among them up to  $n = 2$ , with a mean percentage deviation of 3.0%, being the  $B_1 - B_2$  method and the  $\gamma_z$

coefficient the ones performing the major percentual difference (about 7.0%) among them. For larger values of factor  $n$ , methods P-delta and  $\gamma_z$  coefficient show similar behavior (less than 2% of percentage difference) and become less conservative than the other implemented methods.

It is worth noting that for  $n=3$ , the  $\gamma_z$  coefficient method practically reaches the applicability limit ( $\gamma_z \leq 1.3$ ) recommended by NBR 6118-2014 [9], as well as, the  $B_1 - B_2$  method, that also reaches the applicability limit ( $B_2 \leq 1.4$ ) recommended by NBR 8800:2008 [11], for columns 2 to 6. The Eurocode method only reaches its applicability limit ( $3 \leq \alpha_{cr} < 10$ ) for  $n=5$ , with  $\alpha_{cr} = 2.54$ .

Figure 10 (Load - bending moment relationship) shows overall similarity of results between methods up to  $n=4$ . For  $n=5$ , the  $\gamma_z$  method and the Eurocode method yield the largest results, this is so because the value of the coefficients used in these methods (determined only once for the entire structural system) is also larger than that used in the other approaches.

Figure 11 (column 27) reveals that the axial force values determined by the methods diverge for  $n \geq 4$ . On the other hand, Figure 12 (column 33) presents similar results for all methods. This result shows that second order effects have a lower influence on axial forces than on the bending moment behavior, for example.

The shear force analysis of column 27 shows that MAES diverges from the other methods for  $n \geq 2$ . This can be explained by the fact that MAES does not amplify the shear forces. For column 33, however, the degree of agreement of the results of all methods is acceptable.

## 5 CONCLUSIONS

The subject studied herein has been extensively researched since the 1970s and, considering its relevance, especially for the design of tall and slender structures, it is still challenging for structural engineers and researchers. As such, this paper presented, in a complete and yet simple manner, a comparison between numerous approximate methods with the objective of enriching discussions about this important field of study.

In summary, the presented approximate methods for elastic second-order analysis of structures show a good degree of agreement of results when applied within their recommended applicability limits, in the case of the  $B_1 - B_2$  method ( $B_2 \leq 1.4$ ), the  $\gamma_z$  coefficient ( $\gamma_z \leq 1.3$ ) and the Eurocode 3 method -  $\alpha_{cr}$  factor ( $3 \leq \alpha_{cr} < 10$ ). This study also showed that methods that amplify horizontal loads or include fictitious lateral forces tend to accentuate shear force values, being closer to the those obtained by the geometrically exact analysis.

This closing paragraph is taken as an opportunity to reinforce the limitations of approximate methods. Chen and Toma [18] report that approximate methodologies are recommended only for regular framed structures subjected to regular load distributions. EN 1993-1-1:2005 [13] stresses that the approximate method is acceptable for regular framed structures subject to a regular loading. Dória et al. [19] state that methods based on the ratio  $\Delta_2 / \Delta_1$  are not adequate to assess second-order effects in structures. Instead of the  $B_2$  factor, these authors suggest the  $\alpha_{cr}$  factor, from Eurocode 3, as a more adequate indicator of the importance of second-order effects in structures.

## ACKNOWLEDGEMENTS

The authors would like to thank Capes, CNPq and Fapes for the financial support.

## REFERENCES

- [1] D. M. Oliveira, "Estudo dos processos aproximados utilizados para a consideração das não-linearidades física e geométrica na análise global das estruturas de concreto armado," Ph.D. dissertation, Univ. Fed. Minas Gerais, Belo Horizonte, 2007.
- [2] M. R. Horne, "An approximate method for calculating the elastic critical loads of multi-storey plane frames," *Struct. Eng. J.*, vol. 53, no. 6, pp. 242–248, Jun 1975.
- [3] B. R. Wood, P. F. Adams, and D. Beaulieu, "Column design by P delta method," *J. Struct. Div.*, vol. 102, no. ST2, pp. 411–427, Feb 1976.
- [4] W. J. LeMessurier, "A practical method of second order analysis part 1 – pin jointed systems," *Eng. J.*, vol. 13, pp. 89–96, 1976.
- [5] W. J. LeMessurier, "A practical method of second order analysis part 2 – rigid frames," *Eng. J.*, vol. 14, pp. 49–67, 1977.
- [6] M. Franco, *Problemas de Estabilidade nos Edifícios de Concreto Armado: Publicação Técnica*. São Paulo: Inst. Eng., 1985.
- [7] M. Franco and A. C. Vasconcelos, *Avaliação Prática dos Efeitos de 2º Ordem em Edifícios Altos: Publicação Técnica*. São Paulo: Inst. Eng., 1991.



- [8] A. C. Vasconcelos, "Critérios para dispensa de consideração do efeito de 2ª ordem," in *Reun. An. IBRACON: Colóq. Estabil. Glob. Estrut. Concr. Armado*, São Paulo, 1985.
- [9] Associação Brasileira de Normas Técnicas, *Projeto de Estruturas de Concreto, Procedimento*, NBR 6118, 2014.
- [10] American Institute of Steel Construction, *Manual of Steel Construction-Load and Resistance Factor Design Specification for Structural Steel Buildings*, ANSI/AISC 360-16, 2016.
- [11] Associação Brasileira de Normas Técnicas, *Projeto de Estruturas de Aço e Estruturas Mistas de Aço e Concreto de Edifícios*, NBR 8800, 2008.
- [12] Associação Brasileira de Normas Técnicas, *Projeto de Estruturas de Aço e Estruturas Mistas de Aço e Concreto de Edifícios*, NBR 8800, 1986.
- [13] European Standard, *Design of Steel Structures - Part 1-1. General Rules and Rules for Buildings*, Eurocode 3, 2005. [English version].
- [14] R. L. G. Silva, "Avaliação dos efeitos de 2º ordem em edifícios de aço utilizando métodos aproximados e análise rigorosa," M.S. thesis, Univ. Fed. Minas Gerais, Belo Horizonte, 2004.
- [15] R. D. Ziemian, *Guide to Stability Design Criteria for Metal Structures*. USA: Wiley, 2010.
- [16] A. Rutenberg, "A direct P-delta analysis using standard plane frame computer programs," *Comput. Struct.*, vol. 14, pp. 97–102, Feb 1981.
- [17] E. Wilson and A. Habibullah, "Static and dynamic analysis of multi-story buildings including P-Delta effects," *Earthq. Spectra*, vol. 3, no. 2, pp. 289–298, May 1987.
- [18] W. F. Chen and S. Toma, *Advanced Analysis of Steel Frames*. Boca Raton: CRC Press, 1994.
- [19] A. S. Dória, M. Malite, and L. C. M. Vieira, "On frame stability analysis," in *Proc. Ann. Stab. Conf.*, Missouri, 2013.
- [20] C. Carter, *The Evolution of Stability Provisions in the AISC Specification, Steel Day Eve*. New York: AISC, 2013.
- [21] D. W. White, A. E. Surovek, B. N. Alemdar, C.-J. Chang, Y. D. Kim, and G. H. Kuchenbecker, "Stability analysis and design of steel building frames using the 2005 AISC specification," *Steel Struct.*, vol. 6, pp. 71–91, 2006.
- [22] A. Badke-Neto and W. G. Ferreira, *Dimensionamento de Elementos de Perfis de Aço Laminados e Soldados: Com Exemplos Numéricos*, 3a ed. Vitória: GSS, 2016.
- [23] I. MacPhedran and G. Grondin, "A brief history of beam-column design," in *CSCE Ann. Gen. Meet. Conf.*, Yellowknife, 2007.
- [24] Y. P. Souza et al., *Introdução à Teoria da Estabilidade Elástica - Conceitos, Implementações Computacionais e Aspectos Normativos*. 3a ed. Vitória: LBF, 2018.
- [25] W. B. Ferreira, L. A. R. Luchi and W. G. Ferreira, "Estabilidade de estruturas projetadas com lajes planas protendidas," in *The 7th Int. Struct. Eng. Constr. Conf. – New Develop. Struct. Eng. Constr.*, Honolulu, 2013.
- [26] J. M. Araújo, *Projeto Estrutural de Edifícios de Concreto Armado*, 3a ed. Rio Grande: Dunas, 2014.
- [27] A. C. Avakian, *Estruturas aporticadas mistas aço-concreto: avaliação de metodologias de análise*, M.S. thesis, Univ. Fed. Rio de Janeiro, Rio de Janeiro, 2007.
- [28] Canada Standards Association, *Limits States Design of Steel Structures*, CAN/CSA-S16.1-M94, 1994.
- [29] C. Bernuzzi and B. Cordova, *Structural Steel Design to Eurocode 3 and AISC Specifications*. Oxford: John Wiley & Sons, 2016.
- [30] J.-P. Muzeau, *La Construction Métallique Avec les Eurocodes*. Saint-Denis, France: Afnor et Groupe Eyrolles, 2014.

---

**Author contributions:** LBL: conceptualization, writing, numerical simulation; WGF: conceptualization, writing, data curation, supervision; PMMPCC: writing, data curation, formal analysis; AMCS: data curation, formal analysis, final review.

**Editors:** Sergio Hampshire C. Santos, Guilherme Aris Parsekian.